International Journal of Applied Pharmaceutics

ISSN- 0975-7058 Vol 16, Issue 1, 2024

Original Article

PREPARATION, CHARACTERIZATION AND EVALUATION OF MYRICETIN-LOADED NANOEMULSION FOR THERAPEUTIC EFFICACY IN WOUND HEALING

TANVIR YUSUF SHAIKH, SANTRAM LODHI*

Sri Sathya Sai Institute of Pharmaceutical Sciences, Ram Krishna Dharmarth Foundation University, Gandhi Nagar, Bhopal-462033, Madhya Pradesh, India

***Corresponding author: Santram Lodhi; *Email: srlodhi78@gmail.com**

Received: 08 Apr 2023, Revised and Accepted: 30 Oct 2023

ABSTRACT

Objective: Aim of the present study was the development, optimization and evaluation of myricetin-loaded nanoemulsion gel for wound healing.

Methods: Myricetin nanoemulsion was prepared by selecting Peanut oil as oil (wt %), Tween 20 and Polyethylene glycol 400 as surfactant and cosurfactant (S_{mix}) and aqueous phase water. Performance of nanoemulsion gel was evaluated by wound healing activity tested against wound contraction, hydroxyproline content, protein content and antioxidant assay.

Results: The optimized nanoemulsion (NEF1) exhibited appreciable stability concerning droplet size and PDI when stored at 5 °C, 25 °C and 40°C up to three months. Morphological characterization by TEM indicated a spherical shape. Wound healing effect was observed through a significant ($p<0.5$) increase in hydroxyproline content, protein content and antioxidant status in wound tissue. The level of superoxide dismutase (SOD) and catalase were found to increase significantly in wound tissue after treatment with Myricetin loaded nanoemulsion (MYCT-NE) gel, as well as results were comparable to Betadine cream.

Conclusion: In conclusion, MYCT-NE gel was found potent wound healing effect through the reduction of oxidative stress and epithelialization of tissue.

Keywords: Myricetin, Nanoemulsion, Gel, Tween-20, Polyethylene glycol-400, Wound healing

DOI: https://dx.doi.org/10.22159/ijap.2024v16i1.49112 Journal homepage: https://innovareacademics.in/journals/index.php/ijap

INTRODUCTION

The wound healing is not a simple linear process, which is one of the most complex and dynamic processes that involved with multiple biological pathways, blood elements, cells, growth factors, and extracellular matrix (ECM) [1]. Wound healing process can be facilitated by natural products with their multiple medicinal properties of various chemical families. Each bioactive agent may have specific function on wound healing properties.

Nanoemulsions are metastable colloidal systems consisting on droplets of one liquid dispersed within another immiscible liquid [2]. Nanoemulsions are versatile carriers for local delivery of hydrophilic, lipophilic and amphiphilic molecules. In fact, these systems have arisen as a novel carrier system for improving the bioavailability of poorly absorbed herbs actives/extracts [3, 4]. In the presence of an emulsifier, mixing oil and water creates a coarse emulsion that can transform into a nanoemulsion either naturally or by the use of high energy [5]. FDA-approved and GRAS-certified oils viz. Peanut oil (PO), Triacetin (Glyceryl triacetate), Sefsol 218 (Propylene glycol mono ethyl ether) etc. are preferred over conventional high-density fixed oils such as castor oil, coconut oil, sesame oil, cottonseed oil, fish oil, linseed oil, mineral oil olive oil, peanut oil, sunflower oil etc. [6, 7].

Myricetin belongs to the group of flavonoids known as flavonols. It is chemically 3, 5, 7-Trihydroxy-2-(3, 4, 5-trihydroxy phenyl)-4-chromenone [8, 9]. It has been suggested that myricetin is a more potent antioxidant than quercetin [10, 11]. In both acute and chronic models of inflammation, Wang *et al.* examined the *in vivo* anti-inflammatory effects of myricetin [12]. Myricetin had an inverse relationship with the risk of type II diabetes among different flavonoids, indicating that it may have potential anti-diabetic activity [13, 14]. In mice that fed a high-fat and high-sucrose diet, 0.12 % Myricetin supplementation considerably reduced hypertriglyceridemia and hypercholesterolemia, which raises the possibility that myricetin may have anti-obesity and anti-insulin resistance properties [15]. Through diverse molecular mechanisms, myricetin exhibits anticancer efficacy against different types of cancer.

Natural bioactives are poorly water-soluble, meaning that it is restricted to the superficial stratum corneum (SC) after topical delivery. Though Myricetin is a natural flavonoid and lipid-soluble substances are usually considered to penetrate the stratum corneum fairly rapidly, the absolute water-insolubility of myricetin might justify its poor capability to permeate through stratum corneum. So, approaches to increase drug penetration into the skin have to be researched. The present study was aimed to investigate the potential application of nanoemulsion as a topical carrier system for delivery of the myricetin. Present study consists of the preparation and characterization of nanoemulsion formulation of myricetin and evaluation of prepared nanoemulsion gel for wound healing activity.

MATERIALS AND METHODS

Materials

Myricetin was purchased from Yucca Enterprises, Mumbai. Peanut oil, arachis oil, castor oil, olive oil, Tween-20 (Polyoxyethylene (20) sorbitan monolaurate), Tween-40 (Polyoxyethylene sorbitan monopalmitate), Tween-60 (Polyoxyethylene sorbitan monostearate), Tween-80 (Polyoxyethylene sorbitan monooleate), Span 20 (Sorbitan laurate) (Sorbitan monododecanoate), Span-80 (Sorbitan monooleate) (Sorbitan (2)-mono-a-octadecanoate), Isopropyl alcohol, Polyethylene glycol-400, propylene glycol were procured from Loba Chemie Pvt. Ltd., Mumbai, India. The orthophosphoric acid (HPLC grade 88%), acetonitrile (HPLC grade 99.9%), and methanol (HPLC grade, 99.9%) were obtained from Merck Specialties Pvt Ltd., Mumbai, India. Furthermore, all the other chemicals, reagents, solvents were used in the present study of analytical grade. The water used was deionized by a Milli-Q filtration system (Millipore Corporation, Bedford, MA).

Solubility assessment of myricetin

Excess amount of Myricetin was added into 4 ml of each component (Oil, surfactants, and co-surfactants). Take each oils (Peanut oil, arachis oil, castor oil, coconut oil, olive oil) separately in 5 ml capacity stopper vial, and mixed using vortex mixer. The mixture vials was allowed to equilibrate by shaking at 25±0.5 °C. Then 2 ml

of the solution was withdrawn after 36 h, with centrifugation (13,000 rpm/min, 10 min) followed by filtration using syringe filter. Dilutions were made in methanol and the concentration of myricetin was determined by UV spectrophotometer at 370 nm. Miscibility study was performed by taking equal amount of all components oil, surfactants and co-surfactant and kept for 24 h for visual observation [16].

Six types of surfactants were screened for nanoemulsion formulation, which included Tween-20 (Polysorbate 20), Tween-40 (Polyoxyethylenesorbitan monopalmitate), Tween-60 (Polyoxyethylene sorbitan monostearate), Tween-80 (Polyoxyethylene sorbitan monooleate), Span-20 (Sorbitan monolaurate), Span-80 (Sorbitan monooleate), and Sorbitan monostearate and co-surfactant were Isopropyl alcohol, Polyethylene glycol-400, and Propylene glycol screen for selection. The selected oils and surfactant/co-surfactant were further used for the preparation of pseudo-ternary phase diagrams.

Construction of pseudo-ternary phase diagrams

Surfactant and co-surfactant (S_{mix}) in each group were mixed in different volume ratios (1:0, 1:1, 1:2, 1:3, 2:1, 3:1, 4:1) and the stock of 100 ml of each group was prepared in distilled water. For each phase diagram, oil and specific Smix ratio was mixed thoroughly in different volume ratios from 1:9 to 9:1 in different small glass test tubes. Maximum ratios of oil, each Smix were covered for the study to delineate the boundaries of phases precisely formed in the phase diagrams. To construct pseudoternary phase diagrams, the oil phase (Peanut Oil) was mixed with different ratio of surfactant and cosurfactant (Tween 20 and Polyethylene glycol 400, respectively) and the mixture was titrated with distilled water until it turned turbid. Distilled water was added dropwise at room temperature 25±5 ºC to the oil, and surfactant and co-surfactant mixture.

The samples were vigorously mixed with vortex mixer for 2 min and kept at room temperature 25±5 ºC for 24 h to reach equilibrium. Visual inspection was made after each addition of water and samples were identified as nanoemulsions when they appear as transparent an easily flowable liquid. The three axes of the phase diagram corresponded to the three components of the nanoemulsion system i.e. aqueous, oil, and S_{mix} phases [17, 18]. Pseudoternary phase diagram was prepared by available online software (www.ternaryplot.com).

Preparation of nanoemulsion

On the basis of solubility assessment, surfactant and co-surfactant were selected for preparation of nanoemulsion of Myricetin. Accurate weighed amount of Myricetin (50 mg) was incorporated through a spontaneous emulsification method with slight modification [19]. Organic phase consists of Myricetin dispersed in peanut oil (0.5 ml), whereas aqueous phase contains mixture of tween 20 as surfactant and polyethylene glycol 400 as co-surfactant with best ratio from ternary phase diagram. Organic phase was poured into aqueous phase dropwise, followed by continuous stirring using a magnetic stirrer (IKA India Private Limited, Bengaluru, India) at 5000 rpm for 5 min to obtained the primary emulsion. Further primary emulsions were reduced into nanoemulsion by high presser homogenization (T-25 digital ULTRA-TURRAX®, IKA India Private Limited, India) at 11000 rpm for 20 min. The resulting nanoemulsions were transparent and readily flowable, which was allowed to stand for 2 h for equilibration and then characterized. Different nanoemulsions were selected from the Pseudo-ternary phase diagram for the thermodynamic evaluation study.

Thermodynamic stability studies

Selected formulations were centrifuged at 3500 rpm for 30 min. Those formulations that did not show any phase separations were taken for the heating and cooling cycle.

Six cycles between refrigerator temperatures of 4 ºC and 45 ºC for 48 h were done. The formulations that were stable at these temperatures were subjected to the freeze-thaw cycle test.

Three freeze-thaw cycles were done for the formulations between–21 ºC and+25 ºC. Those formulations that survived thermodynamic stability tests were selected for the further studies [20].

Characterization of prepared nanoemulsions

Determination of globule size, polydispersity index and zeta potential

The mean globule size, polydispersity index, and zeta potential were characterized by using a Malvern Zetasizer (Nano ZS 90, Malvern Ltd., UK). Prior to the measurements, samples (0.1 ml) were diluted with 10 ml of double-distilled water in a volumetric flask mixed with vigorous shaking to produce appropriate scattering intensity. The measurements were made at an angle of 90 ° at 25 ºC [21, 22].

Entrapment efficacy determination

Percentage entrapment efficacy is defined as the amount of drug entrapped within the matrix core formed by the organic phase components. First, the nanoemulsions were centrifuged at 12000 rpm for 20 min, and the supernatant was collected and filtered through a 0.22 µm membrane filter. Then, the drug was quantified using HPLC, and the entrapment efficiency was mentioned as the percentage by using the below-mentioned formula [23].

$$\% \text{ Entrapment efficacy (EE)} = \frac{\text{Amount of drug content}}{\text{The total amount of drug}} \times 100$$

Surface morphology study

The morphology of the prepared nanoemulsion was studied by using a Transmission Electron Microscope (Jeol/JEM 2100, USA). A drop of diluted nanoemulsion (with distilled water) was applied to a carbon-coated copper grid. The negative stain was used with 2% phosphotungstic acid and kept for 30 second. The grid was analyzed using the Transmission Electron Microscope with an accelerating voltage of 60–80 kV [23, 24].

Stability study

Optimized NE was evaluated for stability study at different temperature up to three months as per International Conference on Harmonization (ICH) guidelines. Sufficient quantity of optimized formulations were kept at 40 °C±2 °C/75%±5% RH in a humidity chamber, at room temperature 25 °C±2 °C/60%±5% RH and under refrigeration (5 °C±2 °C). The sample of formulations was withdrawn at 1, 30, 60 and 90 d. Samples of the formulations were analyzed for PDI, droplet size and viscosity. All tests were performed in triplicates of samples.

Preparation of nanoemulsion gel

Prepared nanoemulsions (NE) were converted into gels, using 2.5% of carbopol 934. Optimized nanoemulsion was incorporated in the previously prepared blank carbopol 934 dispersion in distilled water with constant stirring up to 1 h and homogenized vigorously to get gel. It was kept overnight after addition of 2-3 drops of triethanolamine as cross cross-linking agent using constant slow stirring. The final pH was adjusted to 7.4. Mayrecetin-loaded NE gel (0.5%, w/v) was prepared by incorporation of the optimized NE (equivalent to 0.5% w/v drug) in the polymer solution, followed by all similar steps.

Characterization of nanoemulsion gel

Spreadability

An apparatus of wood containing a pulley was used for the study of the spreadability of the prepared nanoemulsion gel formulations. It was comprised of two glass slides: one glass was fixed, and the other glass was allowed to move. A weighted amount (1 g) of the prepared nanoemulsion gel formulation was placed in between the glass slides, and a measured amount of weight was placed on the upper glass slide. The time for the upper glass to cover a distance of 8 cm was noted [25].

pH and viscosity

The pH of the prepared formulations was evaluated using a calibrated pH meter. The viscosity of prepared NE gels was measured at room

temperature using Brookfield viscometer (Brookfield viscometer, USA). A spindle no. 64 was used for evaluating the viscosity of the prepared nanoemulsion gel formulations.

Drug release study

In vitro diffusion study was carried out in a Franz diffusion cell using semipermeable cellophane membrane [26, 27]. Semipermeable cellophane membrane mounted between donor and receiver compartments of the Franz diffusion cell. The receptor cell was filled with phosphate buffer (pH 7.4) and continuously rotated with magnetic stirrer at a speed of 100 rpm. Formulation applied through donor compartment on the dialysis membrane. The system was adjusted at 37±0.5 ℃. Aliquots (0.5 ml) were withdrawn at specific time intervals and replaced with same volume of fresh buffer solution of pH 7.4. The samples were measured spectrophotometrically at 370 nm against phosphate buffer (pH 7.4) as a blank. The cumulative amount of drug release was calculated. All experiments were repeated for three times and mean values were calculated.

***In vivo* study for wound healing activity**

Animal and treatment protocol

Inbreed house wistar rats (200–250 g) of either sex were acclimatized to laboratory hygienic circumstances for 10 d early of the experiment. The animals were fed a commercial pellet diet (Hindustan Lever Pvt, Bangalore, India), and water ad libitum. All animal experimentation was performed with the approval of the Institutional Animal Ethical Committee (Reg. No. 1546/PO/E/S/11/CPCSEA). Animals were divided into three groups consisting of six animals each group. The control group received vehicle (without Myrecetin loaded NE gel), test group received 370 nm Myrecetin loaded NE (MYCT-NE) gel and the reference group received marketed formulation Betadine cream (Win-Mdicare Pvt. Ltd. New Delhi, India). All treatments were given topically.

Dead space wound model

Dead space wound model is used for the study of granuloma tissue formation. The wound healing effect was assessed by measurement of dry granulation weight, estimation of biochemical parameters and histological study [28]. Animals were anaesthetized by light ether and wound was made by implantation of a polypropylene tube (2.0 x 0.5), on either side, in the lumber region on the dorsal surface of animals. On the 9th post-wounding day, granuloma tissue formed on implanted tube was dissected out carefully. Granuloma tissue from tubes was dried (60 °C) and stored in 10% formalin for the biochemical parameters. Wound tissue was used for histopathological studies. Biochemical assessment e. g. protein content, hydroxyproline content, and antioxidants level in the granuloma tissues were determined by standard reported methods.

Hydroxyproline estimation

Granuloma tissues collected on 9th day from each group and one part of tissue was analyzed for hydroxyproline content that is a basic constituent of collagen. Tissues were dried at 60–70 °C up to constant weight and samples were hydrolyzed with 6N HCl for 4 h at 130 °C. The hydrolysate was neutralized then subjected to Chloramine-T oxidation for 20 min. The colored adduct formed with Ehrlich reagent at 60 °C was analyzed at 557 nm using a spectrophotometer [29]. Standard hydroxyproline was also run and values reported as mg/g of dry weight of tissue.

Protein estimation

On the post wounding days 9th, the protein content of skin tissues were determined by method of Lowry *et al.* [30]. The tissue lysate was treated with a mixture of sodium tartrate, copper sulphate and sodium carbonate. The mixture was left to stand for 10 min and then treated with Folin-Ciocalteau reagent, which gives a bluish color in 20–30 min. The absorbance was taken at 650 nm using a Spectrophotometer.

Antioxidant assay

The granuloma tissues were collected from each animal group and analyzed for antioxidant assay. Catalase was estimated following the breakdown of hydrogen peroxide according to the method of Beers and Sizer (1952) [31]. Superoxide dismutase (SOD) was assayed according to Misra and Fridovich (1972) [32] based on the inhibition of epinephrine autoxidation by the enzyme. Reduced glutathione (GSH) level was determined by method of Moron *et al.* (1979) [33]. Tissue homogenates were immediately precipitated with 0.1 ml of 25% TCA and separated by centrifugation. The assay of free-SH groups in 3 ml of sample was done by the addition of 2 ml of 0.6 mmol DTNB and 0.9 ml 0.2 mmol sodium phosphate buffer (pH 8.0) to 0.1 ml of the supernatant and the absorbance was read at 412 nm using a UV-spectrophotometer.

Histopathological study

Animals were anaesthetized before taking skin sample using diethyl ether. On 9th day wound tissue sample from each group were collected. One part of tissue sample were fixed in 10% buffered formalin, processed, blocked with paraffin and then cut into 6 µm thickness sections and stained with hematoxylin and eosin (HE) stains [34]. The tissues were examined by light microscope for internal structure of tissue.

Statistical analysis

Data are presented as the mean±standard deviation. Treated groups were compared with the control and standard group. The results were analyzed statistically by one way analysis of variance (ANOVA) using GraphPad Prism 5 software. The results were considered statistically significant at $p<0.05$.

RESULTS AND DISCUSSION

Solubility assessment

Solubility of Myricetin was determined in various oil, surfactant and co-surfactants (table 1). The ability of nanoemulsion to maintain the drug in solubilized form is greatly influenced by solubility of drug in oil phase. If the surfactant or co surfactant is contributing to drug solubilization, there could be a risk of precipitation, particularly when oral or parenteral nanoemulsion is preferred. There is a dilution of nanoemulsion in the gastrointestinal tract can lead to a lowering of the solvent capacity of the surfactant or co-surfactant.

Table 1: Myricetin solubility in different oils, surfactants and co-surfactants

S. No.	Oils	Solubility (mg/ml)
1	Peanut oil	14.15±0.59
2	Arachis Oil	12.13±0.18
3	Castor Oil	3.9±0.13
4	Coconut Oil	8.11±0.32
5	Olive Oil	5.46±0.11
	Surfactants	Solubility (mg/ml)
1	Tween 20	16.41±0.03
2	Tween 40	15.01±0.06
3	Tween 60	10.73±0.05
4	Tween 80	5.61±0.17
5	Span 20	2.17±0.06
6	Span 80	1.73±0.04
	Co Surfactants	Solubility (mg/ml)
1	Isopropyl alcohol	39.41±0.13
2	Polyethylene glycol 400	40.18±0.21
3	Propylene glycol	13.59±0.11

Data represent as mean±SD n =5

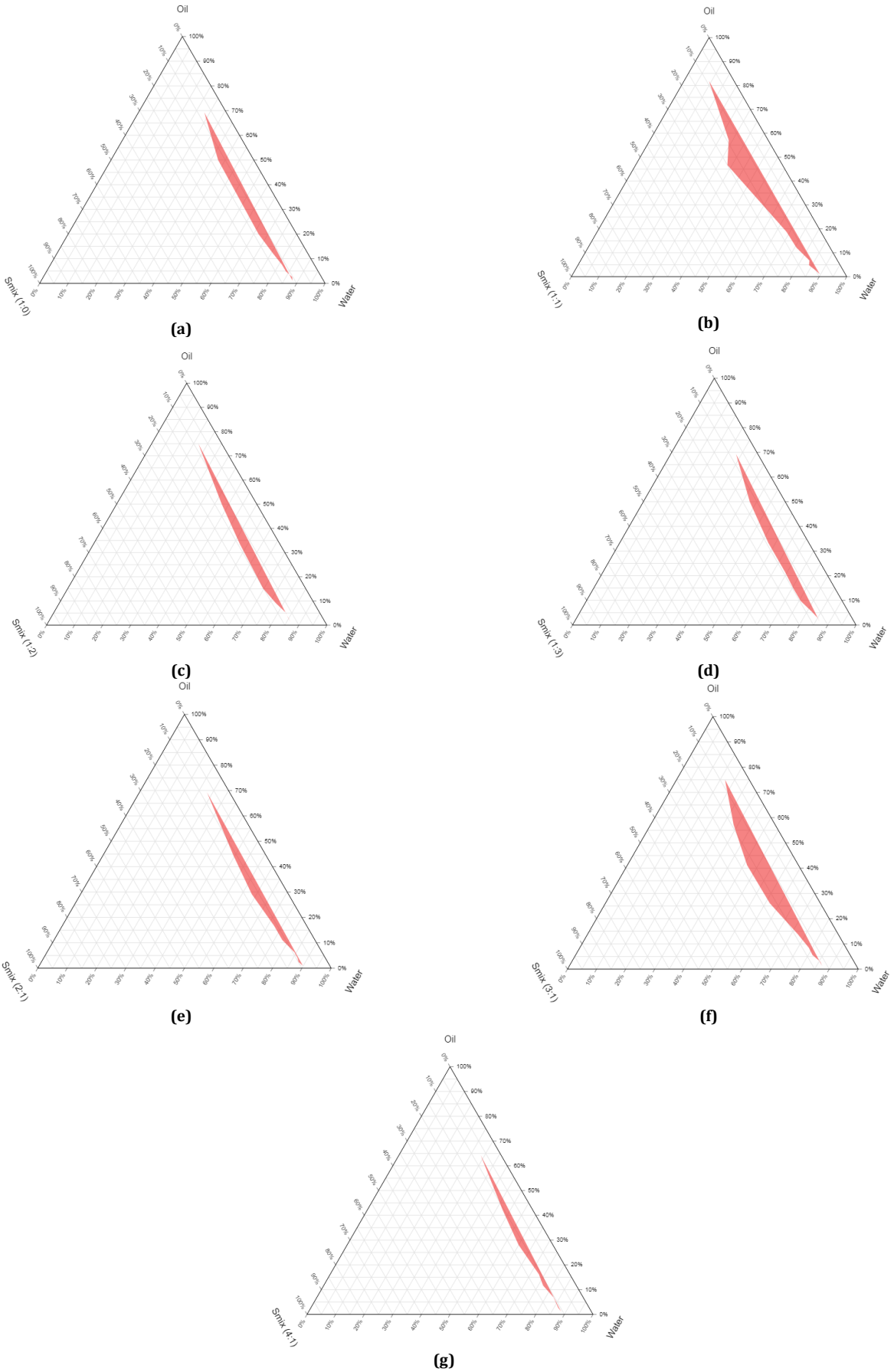

Fig. 1: Ternary phase diagrams of nanoemulsions consisting of peanut oil with different ratio of surfactant and co-surfactants (Smix ratio) and water. (a) 1:0; (b) 1:1; (c) 1:2; (d) 1:3; (e) 2:1; (f) 3:1; (g) (4:1)

Lipophilic drugs are soluble in o/w nanoemulsion. The solubility of myricetin was found to highest in Peanut oil (14.15±0.59 mg/ml). The peanut oil was selected as oil phase for the development of nanoemulsion. Large amount of surfactants may cause gastrointestinal and skin irritation when administered orally and topically, respectively. Non-ionic surfactants are less toxic [35]. The surfactants were screened in a wide range of HLB values (4.3 to 17). From the series of surfactant, the order of emulsifying ability of surfactant with Peanut oil was as Tween20>Tween40>Tween60>Tween80>Span20>Span80. The percent emulsification of Peanut oil by Tween 20 was higher due to a higher HLB value, so it was selected as the primary surfactant. The solubility of Polyethylene glycol-400 with the Myrecetin was observed higher than the other co-surfactants. The co-surfactant was selected to reduce the interfacial tension and produce a larger NE region in the constructed phase diagrams. Co-surfactants are added to obtain nanoemulsion should be at low surfactant concentrations [36].

Effect of surfactant and co-surfactant ratio (S_{mix}) on nanoemulsion formulation

The ternary phase diagram was constructed by using peanut oil as oil phase, Tween 20 as surfactant and Propylene glycol-400 as co-surfactant and water (fig. 1). The Tween-20 and Polyethylene glycol-400 were added to the peanut oil and were titrated against the aqueous phase. The transparent region obtained in the phase diagrams indicated the nanoemulsion region. The rest of the region on the phase diagram represents the turbid and conventional emulsion. The effect of the S_{mix} ratio was assessed further to optimize the nanoemulsion system. When Tween 20 was used without co-surfactant, a low nanoemulsion area was observed. It shows that Tween 20 alone could not reduce the interfacial tension between the oil and water face and the addition of a co-surfactant is necessary. If co-surfactant was added with surfactant in equal amounts S_{mix} 1:1, a higher nanoemulsion region was observed because of reduction in interfacial tension and increased fluidity of interface. When surfactant concentration increased from 2:1 to 3:1 nanoemulsion region was higher but less than ratio 1:1 and, showing the optimum emulsification was achieved. If co-surfactant, Polyethylene glycol 400 concentrations was increased with respects to surfactant Tween 20 the S_{mix} 1:2, S_{mix} 1:3 nanoemulsion area was decreased as compare to S_{mix} 1:1. It may be due to a decrease in surfactant concentration by the increased co-surfactant. There should be optimum concentration of surfactant that will give maximum flux, because high concentration of surfactant decreases the thermodynamic activity of the drug in vehicle and affinity of drug for vehicle becomes greater [37].

Selection of stable nanoemulsion through thermodynamic stability studies

Different nanoemulsion formulations (NEF) were obtained with the help of pseudoternary phase diagrams using different Smix ratio 1:0, 1:1, 1:2, 1:3, 2:1, 3:1, and 4:1. Out of all these formulations, some NE formulations with ratio of 1:1, 2:1, 3:1, and 4:1 were showing higher NE region and good emulsification. All these formulations were screen for thermodynamic stability. All four NE formulations NEF1, NEF2, NEF3 and NEF4 were remains stable, and not shown any phase separation during heating cooling cycle and freeze-thaw cycles.

Table 2: Compositions of oil, Smix and water for selected nanoemulsion formulations

Nanoemulsion formulations	Ingredients (% v/v)			Surfactant/Co-surfactant ratio
	Oil	S_{mix}	Distilled water	
NEF1	12	18	70	1:1
NEF2	10	22	68	2:1
NEF3	14	20	66	3:1
NEF4	10	16	74	4:1

Characterization of prepared nanoemulsion

Determination of globule size, polydispersity index and zeta potential

All nanoemulsion formulation code NEF1 to NEF4 was subjected to the droplet size analysis, zeta potential determination, polydispersity index and entrapment efficiency. Results were showed that droplet size was increased with an increase in the concentration of peanut oil. Less than 100 nm droplet size of nanoemulsion was considered an appropriate formulation. These data also confirmed by surface morphology analysis of nanoemulsion formulations. Mean droplet size of NEF1 was 83.57±2.95. Other formulations showed droplet size higher than NEF1 formulation that is not appropriate. The polydispersity was at a minimum in the case of NEF1, which contained S_{mix} ratio 1:1, suggesting uniformity of droplet size in the formulation.

The importance of the zeta potential evaluation is due to its relation to the stability of colloidal dispersions. If zeta potential value in modulus is small, the attraction between the droplets is greater than the repulsion, which can lead to the flocculation and breakage of the dispersion. The NEF1 presented mean value of zeta potential is-29.26±0.86 mV for the formulation, which indicates a good physical stability. Entrapment efficiency of optimized formulation NEF1 was found to be 92.74±1.52% that is higher than the other NEF2, NEF3 and NEF4 formulations.

Table 3: Observation of selected stable nanoemulsions with their droplet size, polydispersity index, zeta potential and entrapment efficiency

Formulation code	Mean droplet size (nm)	Polydispersity Index	Zeta potential (mV)	Entrapment efficiency (%)
NEF1	83.57±2.95	0.125±0.07	-29.26±0.86	92.74±1.82
NEF2	101.62±3.68	0.172±0.04	-18.45±0.52	76.18±1.37
NEF3	135.84±3.55	0.192±0.09	-11.63±0.49	71.35±1.50
NEF4	124.20±3.08	0.218±0.18	-17.55±0.78	59.48±1.64

Data represent as mean±SD n =5

Surface morphological study by transmission electron microscopy (TEM)

The TEM microphotographs of myricetin-loaded nanoemulsion (MYCT-NE) indicated that the droplets were spherical with nanosized globule (fig. 2). The droplets in the nanoemulsion appear as dark and the surroundings are bright. The diameter of globules was found to be around 83 nm.

Stability study of optimized nanoemulsion formulation

Nanoemulsion remains transparent all over the stability period. No formulation showed turbidity or, precipitate or breakdown of the emulsified structure. The stability study showed no significance change in size and PDI during 90 d. The droplet size and PDI remains stable. It was concluded that NEF1 was stable with respect to size and PDI during 90 d. These results indicated that optimized formulation is

stable as there were no significant changes in physical parameters and can be recommended for topical application in drug delivery system.

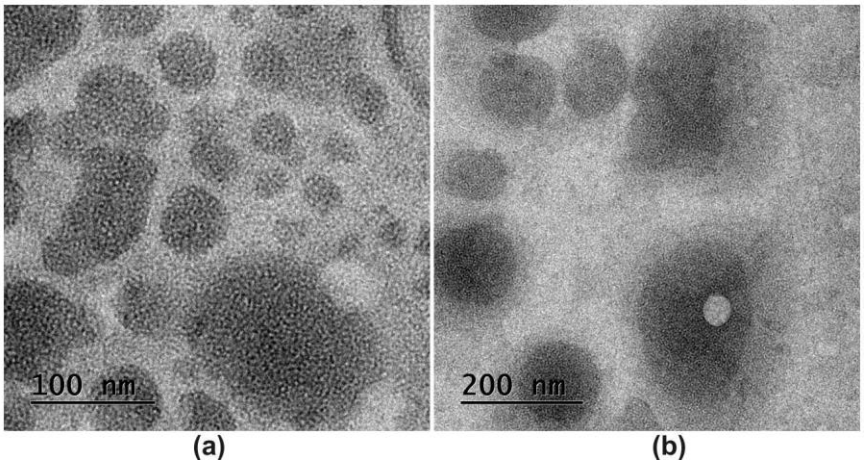

Fig. 2: Transmission electron microscopy of nanoemulsion prepared with S_{mix} ratio 1:1 (NEF1): (a) Scale bar is 100 nm; (b) Scale bar is 200 nm

Table 4: Stability study of optimized nanoemulsion (NEF1) batch for droplet size (nm), PDI at different time period and temperatures

Temperature	Time (days)	Size (nm)	PDI
5 °C	T_1	83.16±1.48	0.127±0.11
	T_{30}	84.79±2.04	0.124±0.12
	T_{60}	84.27±1.55	0.118±0.13
	T_{90}	85.42±1.94	0.125±0.14
25 °C	T_1	83.16±1.14	0.121±0.07
	T_{30}	85.72±1.73	0.119±0.11
	T_{60}	85.46±1.28	0.121±0.21
	T_{90}	86.38±2.05	0.117±0.13
40 °C	T_1	83.28±1.48	0.118±0.01
	T_{30}	85.41±2.13	0.119±0.04
	T_{60}	85.38±2.16	0.119±0.06
	T_{90}	86.07±1.98	0.120±0.04

Data represent as mean±SD n =5

Preparation and characterization of nanoemulsion gel

Optimized nanoemulsion formulation NEF1 was converted into nanoemulsion gel (NE gel) using carbopol 934 polymer. Prepared NE gel was evaluated for spreadability, pH, viscosity and drug release study. Spreadability is another important parameter of gel that can affect to therapeutic efficacy of topical formulation. The appropriate spreadability of any topical formulation is support to the easy application on the skin. The optimized MYCT-NE gel formulations showed spreadability values of 13.55±0.57 g. cm/s that was comparable to the spreadability of market formulation (12.35±0.85).

The actual measured pH of Myrecetin loaded nanoemulsion (MYCT-NE) gel was found as 7.25±0.08. The pH was found appropriate for topical application and it is physiologically compatible with the pH of the skin. Non-irritant and non-allergic property is the primary requirement of suitable topical formulation, pH of the formulation should be compatible to the skin.

Viscosity is a crucial factor in the preparation of transdermal drug delivery. The viscosity of the topical preparation has a direct impact on drug release, spreadability, stability, and ease of application on the site. The polymers and excipients used in the formulations of topical applications also influence their viscosity [2]. The results of the viscosity measurement of MYCT-NE gel at various shear rates, showed that there was an inverse relationship between shear rate and viscosity of gel (table 5 and fig. 3). It was clear that as the shear rate increased the viscosity of gel decreased and vice versa. Decrease in viscosity of MYCT-NE gel with respect to the increase in shear rate, indicates that the gel showed pseudo-plastic flow behavior due to the typical shear thinning nature.

Table 5: Viscosity measurement of prepared Myrecetin loaded nanoemulsion (MYCT-NE) gel formulation

Shear rate (rpm)	Viscosity (cps)
0	62430±124.05
10	34150±110.42
20	21640±104.21
30	13820±91.27
40	11730±81.33
50	10290±75.41

n=5, Data represented as mean±SD.

Cumulative drug release

Drug release study of optimized nanoemulsion (NE) and MYCT-NE gel was performed at 37±0.5 °C at different time interval. Results were shown that the initial release of NE was higher and MYCT-NE gel was slow (table 6 and fig. 3). After 2h, the percentage release of NE was increased gradually up to 48.43±0.75 but MYCT-NE gel was showed only 18.62±0.37. Drug was completely released from NE after 10 h, but gel was shown only 74.21±0.86 release of drug in 10 h. This pattern of release may be due to smaller globule size and larger surface area to release of the drug. Initial drug release from gel was slow due to release from oil layer then release from polymer.

Table 6: Percentage drug release from optimized drug-loaded nanoemulsion (NE) and nanoemulsion gel

Time (h)	Drug release (%)	
	MYCT-NE	MYCT-NE gel
2	48.43±0.75	18.62±0.37
4	74.25±0.14	39.85±0.41
6	85.64±1.20	58.46±0.85
8	91.27±1.64	69.62±0.69
10	99.40±1.58	74.21±0.86
12	99.76±1.84	78.34±0.79
14	99.89±1.95	81.44±0.88

Data represent as mean±SD. n =5

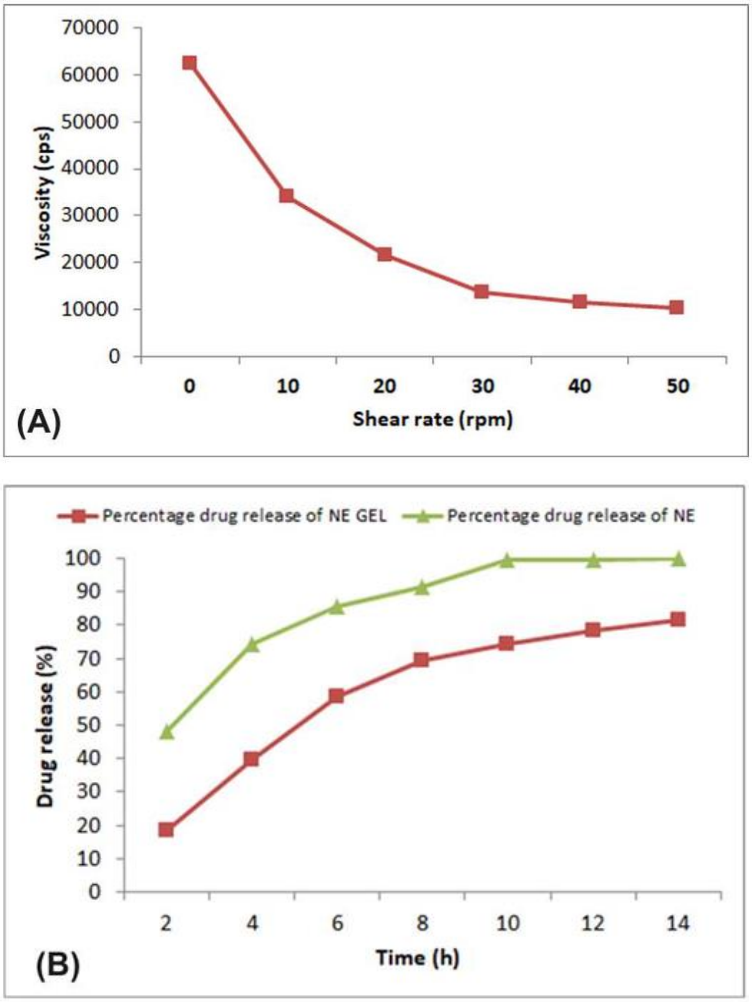

Fig. 3: (A) Viscosity of prepared myrecetin-loaded nanoemulsion (MYCT-NE) gel formulation (B) Percentage drug release from optimized drug-loaded nanoemulsion (NE) and naoemulsion gel

***In vivo* wound healing effect**

Protein content and hydroxyproline level measurement

The protein content of Myricetin-loaded nanoemulsion was 71.69±1.05 and the reference group was 72.18±1.13 (table 7), found to be significantly greater than control group (43.22±0.77). The protein content of wound tissue indicates the level of protein synthesis as well as cellular proliferation and granuloma tissue formation. Increase in protein content of the treated wounds compared to control group suggest that Myricetin stimulates cellular proliferation through an unknown mechanism. Protein synthesis is essential for granuloma tissue formation. Inflammation phase involves neutrophils and fibroblast infiltration of macrophages proliferations which are the basic sources of tissue formation [38].

The hydroxyproline level of NEF1 Myricetin loaded nanoemulsion (30.64±0.46) was found to significantly increased when compared to control group (14.25±0.58). Collagen is the important constituent of the extracellular matrix and major constituent that contribute to wound strength. Hydroxyproline and its peptides are produced after the breakdown of collagen [28]. So, the estimation of hydroxyproline is used as an index for collagen turnover. The new synthesized collagen molecules are laid down at wound side and occurring cross-linking to form fibers. The wound strength is acquired by remodeling of collagen and the formation of intra and inter molecular cross link. Increase hydroxyproline level of Myricetin-loaded nanoemulsion treated wound was indicated increased collagen turnover and this lead to rapid healing of treated wounds.

Table 7: Effect of myricetin-loaded nanoemulsion on biochemical parameters of wound tissue in dead space wound model

Animal groups	Protein content (mg/g tissue)	Hydroxyproline (mg/g tissue)	Dry granuloma weight (mg)
Vehicle control	43.22±0.77	14.25±0.58	26.45±0.70
Myricetin loaded nanoemulsion gel	71.69±1.05*	30.64±0.46*	78.32±0.68*
Betadine cream (Reference)	72.18±1.13*	31.27±0.78*	77.51±0.84*

n= 6 albino rats per group; value represents as mean±SD *p<0.05, when compared each treated group with control group

Antioxidant status

Myricetin-loaded nanoemulsion possess a potent antioxidant effect by an increase in SOD level (21.66±0.42µg/50 mg tissue), GSH (23.54±0.27 µmol/50 mg tissue) and catalase level (28.45±0.25 µmol/50 mg tissue) of wound tissues after 9th day of the healing process (table 8). The significant improvement in SOD, GSH and CAT level in Myricetin loaded nanoemulsion and reference were confirmed that antioxidant effect of myricetin may be one of the healing mechanism of wound.

Reduced glutathione is a strong free radical scavenger. The depletion of GSH results in enhanced lipid peroxidation. This can cause increased GSH utilization and can be correlated to the increase in the level of oxidized glutathione [39]. Treatment with Myricetin loaded nanoemulsion results an increase in GSH levels, which protect the cell membrane against oxidative damage by control the redox status of protein in the membrane. SOD and CAT are enzymes play a significant role in providing antioxidant defenses to an organism that destroys the peroxides. The functions of all enzymes are interconnected. The lowering of enzymes activities results the accumulation of lipid peroxides and increased oxidative stress in wounded site.

Histopathological observations

Histopathological examination of stained sections from different treatment groups were exhibited different healing conditions of the wounded tissues. The results provide good evidence of the suitability of the nanoemulsion formulation for promoting healing and granuloma tissue formation. The observations showed that the original tissue regeneration was found efficiently in the wound treated with Myricetin-loaded nanoemulsion gel (fig. 4B) and reference group without any edema and congestion (fig. 4C). Both group showed proliferation of epithelial tissue covering the wound area. In the vehicle control group, the dermal remodeling process was very slow, which was confirmed by the lower epithelialization time (fig. 4A). The granulation tissue section of control animals showed lower epithelialization, fibrosis and aggregation of macrophages with less collagen fibers, indicating incomplete healing of wounds (fig. 4A). Histopathological studies, confirms increased collagen fibers and fibroblast cells growth.

Table 8: Effect of myricetin-loaded nanoemulsion on antioxidant status of wound tissues in dead space wound model

Animal groups	SOD (µg/50 mg tissue)	CAT (µmol/50 mg tissue)	GSH (µmol/50 mg tissue)
Vehicle control	13.28±0.16	18.32±0.19	12.74±0.08
Myricetin loaded nanoemulsion gel	21.66±0.42*	28.45±0.25*	23.54±0.27*
Betadine cream (Reference)	23.57±0.51*	29.64±0.34*	22.96±0.51*

n= 6 albino rats per group; value represents as mean±SD *p<0.05, when compared each treated group with control group

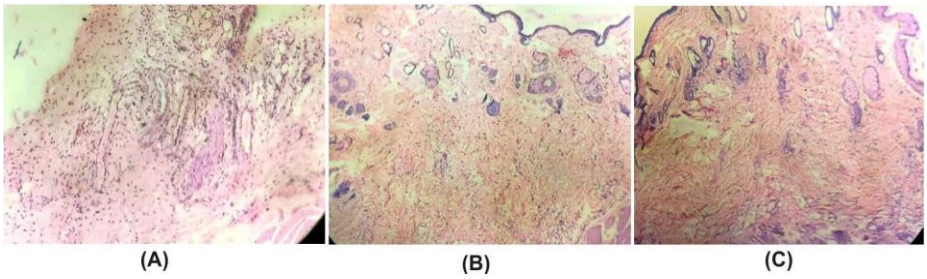

Fig. 4: Photomicrograph of histological observation of wound tissue from dead space wound model: (A) Vehicle control; (B) Myricetin loaded nanoemulsion gel; (C) Betadine cream (Standard)

Myricetin showed antibacterial effects against methicillin-resistant *Staphylococcus aureus*, multidrug-resistant *Burkholderia cepacia*, vancomycin-resistant enterococci, and other medically important organisms such as *Klebsiella pneumoniae* and *Staphylococcus epidermidis* with minimum inhibitory concentrations (MIC) of 32–256 µg/ml [40]. Myricetin also has been proposed as a stronger antioxidant agent [10]. These reports would be support for wound wound-healing potential of myricetin in the present study.

CONCLUSION

The optimized myricetin-loaded nanoemulsion was converted in gel using carbopol 934 and results were showed that it can be used as good carrier for myricetin and exhibited good stability. The myricetin-loaded nanoemulsion gel showed a significant wound healing effect with reduced oxidative status in dead space wound model. The results of the study showed enhanced rate of wound contraction and reduced healing time in animals treated with myricetin-loaded nanoemulsion. Flavonoids are used for numerous therapeutic benefits such as antioxidant, antifungal, antimicrobial, anti-inflammatory and wound healing as already reported. In conclusion, the myricetin-loaded nanoemulsion gel was effectively stimulates wound contraction increased collagen maturation in wound tissues. The collagen maturation was improved may be due to increased cross-linking. Hence the findings suggested that nanoemulsion gel may use as suitable topical delivery carrier for myricetin.

ACKNOWLEDGEMENT

Authors are grateful to Diya Laboratory, Mumbai (MS), India, for providing a formulation analysis facility.

FUNDING

Nil

AUTHORS CONTRIBUTIONS

All the authors have contributed equally.

CONFLICT OF INTERESTS

Declared none

REFERENCES

1. Barrientos S, Stojadinovic O, Golinko MS, Brem H, Tomic Canic M. Growth factors and cytokines in wound healing. Wound Repair Regen. 2008;16(5):585-601. doi: 10.1111/j.1524-475X.2008.00410.x, PMID 19128254.
2. Latif MS, Nawaz A, Asmari M, Uddin J, Ullah H, Ahmad S. Formulation development and *in vitro*/*in vivo* characterization of methotrexate-loaded nanoemulsion gel formulations for enhanced topical delivery. Gels. 2022;9(1):3. doi: 10.3390/gels9010003, PMID 36661771.
3. Maha HL, Sinaga KR, Sinaga KR, Masfria M, Masfria M. Formulation and evaluation of miconazole nitrate nanoemulsion and cream. Asian J Pharm Clin Res. 2018;11(3):319-21. doi: 10.22159/ajpcr.2018.v11i3.22056.
4. Amin N, Das B. A review on formulation and characterization of nanoemulsion. Int J Curr Pharm Sci. 2019;11(4):1-5. doi: 10.22159/ijcpr.2019v11i4.34925.
5. Shakeel F, Baboota S, Ahuja A, Ali J, Shafiq S. Celecoxib nanoemulsion: skin permeation mechanism and bioavailability assessment. J Drug Target. 2008;16(10):733-40. doi: 10.1080/10611860802473402, PMID 18985507.
6. Shakeel F, Ramadan W. Transdermal delivery of anticancer drug caffeine from water-in-oil nanoemulsions. Colloids Surf B Biointerfaces. 2010;75(1):356-62. doi: 10.1016/j.colsurfb.2009.09.010, PMID 19783127.
7. Abulfadhel JN, Al-Shaibani KMH, Al-Gburi KTKA. Original article design and characterization of candesartan cilexetil oral nanoemulsion containing garlic oil. Int J Appl Pharm. 2019;11:116-24.
8. Ono K, Nakane H, Fukushima M, Chermann JC, Barre Sinoussi F. Differential inhibitory effects of various flavonoids on the activities of reverse transcriptase and cellular DNA and RNA polymerases. Eur J Biochem. 1990;190(3):469-76. doi: 10.1111/j.1432-1033.1990.tb15597.x, PMID 1695572.
9. Sato M, Murakami K, Uno M, Nakagawa Y, Katayama S, Akagi K. Site-specific inhibitory mechanism for amyloid β42 aggregation by catechol-type flavonoids targeting the lys residues. J Biol Chem. 2013;288(32):23212-24. doi: 10.1074/jbc.M113.464222, PMID 23792961.
10. Oyama Y, Fuchs PA, Katayama N, Noda K. Myricetin and quercetin, the flavonoid constituents of ginkgo biloba extract, greatly reduce oxidative metabolism in both resting and Ca(2+)-loaded brain neurons. Brain Res. 1994;635(1-2):125-9. doi: 10.1016/0006-8993(94)91431-1, PMID 8173947.
11. Gordon MH, Roedig Penman A. Antioxidant activity of quercetin and myricetin in liposomes. Chem Phys Lipids. 1998;97(1):79-85. doi: 10.1016/s0009-3084(98)00098-x, PMID 10081150.
12. Wang P, Bai HW, Zhu BT. Structural basis for certain naturally occurring bioflavonoids to function as reducing co-substrates of cyclooxygenase I and II. PLOS ONE. 2010;5(8):e12316. doi: 10.1371/journal.pone.0012316, PMID 20808785.
13. Zamora Ros R, Forouhi NG, Sharp SJ, Gonzalez CA, Buijsse B, Guevara M. Dietary intakes of individual flavanols and flavonols are inversely associated with incident type 2 diabetes in European populations. J Nutr. 2014;144(3):335-43. doi: 10.3945/jn.113.184945, PMID 24368432.
14. Yang ZJ, Wang HR, Wang YI, Zhai ZH, Wang LW, Li L. Myricetin attenuated diabetes-associated kidney injuries and dysfunction via regulating nuclear factor (erythroid-derived 2)-like 2 and nuclear factor-κB signaling. Front Pharmacol. 2019;10:647. doi: 10.3389/fphar.2019.00647, PMID 31244660.
15. Choi HN, Kang MJ, Lee SJ, Kim JI. Ameliorative effect of myricetin on insulin resistance in mice fed a high-fat, high-sucrose diet. Nutr Res Pract. 2014;8(5):544-9. doi: 10.4162/nrp.2014.8.5.544, PMID 25324935.
16. Syed HK, Peh KK. Identification of phases of various oil, surfactant/ co-surfactants and water system by ternary phase diagram. Acta Pol Pharm. 2014;71(2):301-9. PMID 25272651.
17. Azeem A, Rizwan M, Ahmad FJ, Iqbal Z, Khar RK, Aqil M. Nanoemulsion components screening and selection: a technical note. AAPS PharmSciTech. 2009;10(1):69-76. doi: 10.1208/s12249-008-9178-x, PMID 19148761.
18. Puppala RK, A VL. Optimization and solubilization study of nanoemulsion budesonide and constructing pseudoternary phase diagram. Asian J Pharm Clin Res 2018;12(1):551-3. doi: 10.22159/ajpcr.2018.v12i1.28686.
19. Back PI, Balestrin LA, Fachel FNS, Nemitz MC, Falkembach M, Soares G. Hydrogels containing soybean isoflavone aglycones-rich fraction-loaded nanoemulsions for wound healing treatment-*in vitro* and *in vivo* studies. Colloids Surf B Biointerfaces. 2020;196:111301. doi: 10.1016/j.colsurfb.2020.111301, PMID 32871442.
20. Shafiq-un-Nabi S, Shakeel F, Talegaonkar S, Ali J, Baboota S, Ahuja A. Formulation development and optimization using nanoemulsion technique: a technical note. AAPS PharmSciTech. 2007;8(2):28. doi: 10.1208/pt0802028, PMID 17622106.
21. Parveen R, Baboota S, Ali J, Ahuja A, Vasudev SS, Ahmad S. Oil based nanocarrier for improved oral delivery of silymarin: *in vitro* and *in vivo* studies. Int J Pharm. 2011;413(1-2):245-53. doi: 10.1016/j.ijpharm.2011.04.041, PMID 21549187.
22. Suciati T, Aliyandi A, Satrialdi. Development of transdermal nanoemulsion formulation for simultaneous delivery of protein vaccine and artin-m adjuvant. Int J Pharm Pharm Sci. 2014;6(6):536-46.
23. Gokhale JP, Mahajan HS, Surana SJ. Quercetin loaded nanoemulsion-based gel for rheumatoid arthritis: *in vivo* and *in vitro* studies. Biomed Pharmacother. 2019;112:108622. doi: 10.1016/j.biopha.2019.108622, PMID 30797146.
24. Gardouh AR, Faheim SH, Noah AT, Ghorab MM. Influence of formulation factors on the size of nanostructured lipid carriers and nanoemulsions prepared by high shear homogenization. Int J Pharm Pharm Sci. 2018;10(4):61-75. doi: 10.22159/ijpps.2018v10i4.23142.
25. Yeo E, Yew Chieng CJ, Choudhury H, Pandey M, Gorain B. Tocotrienols-rich naringenin nanoemulgel for the management of diabetic wound: fabrication, characterization and comparative *in vitro* evaluations. Curr Res Pharmacol Drug Discov. 2021;2:100019. doi: 10.1016/j.crphar.2021.100019, PMID 34909654.
26. Pushpalatha R, Selvamuthukumar S, Kilimozhi D. Cross-linked, cyclodextrin-based nanosponges for curcumin delivery-physicochemical characterization, drug release, stability and cytotoxicity. J Drug Deliv Sci Technol. 2018;45:45-53. doi: 10.1016/j.jddst.2018.03.004.
27. Mathew R, Varkey J. Formulation and *in vitro* evaluation of self nano emulsifying drug delivery system of quercetin for enhancement of oral bioavailability. Int J Curr Pharm Sci. 2022;14(1):60-9. doi: 10.22159/ijcpr.2022v14i1.44113.
28. Lodhi S, Pawar RS, Jain AP, Singhai AK. Wound healing potential of *Tephrosia purpurea* (Linn.) pers. in rats. J Ethnopharmacol. 2006;108(2):204-10. doi: 10.1016/j.jep.2006.05.011, PMID 16806763.
29. Woessner JF. The determination of hydroxyproline in tissue and protein samples containing a small portion of this imino acid. Arch Biochem Biophys. 1961;193:440-7.
30. Lowry OH, Rosebrough NJ, Farr AL, Randall RJ. Protein measurement with the Folin phenol reagent. J Biol Chem. 1951;193(1):265-75. doi: 10.1016/S0021-9258(19)52451-6, PMID 14907713.
31. Beers RF, Sizer IW. A spectrophotometric method for measuring the breakdown of hydrogen peroxide by catalase. J Biol Chem. 1952;195(1):133-40. doi: 10.1016/S0021-9258(19)50881-X, PMID 14938361.
32. Misra HP, Fridovich I. The role of superoxide anion in the autoxidation of epinephrine and a simple assay for superoxide dismutase. J Biol Chem. 1972;247(10):3170-5. doi: 10.1016/S0021-9258(19)45228-9, PMID 4623845.
33. Moron MS, Depierre JW, Mannervik B. Levels of glutathione, glutathione reductase and glutathione S-transferase activities in rat lung and liver. Biochim Biophys Acta. 1979;582(1):67-78. doi: 10.1016/0304-4165(79)90289-7, PMID 760819.

34. Varshney AC, Sharma DN, Singh M, Sharma SK, Nigam JM. Therapeutic value of bovine saliva in wound healing: a histomorphological study. Indian J Exp Biol. 1997;35(5):535-7. PMID 9378522.
35. Kawakami K, Yoshikawa T, Hayashi T, Nishihara Y, Masuda K. Microemulsion formulation for enhanced absorption of poorly soluble drugs. II. *In vivo* study. J Control Release. 2002;81(1-2):75-82. doi: 10.1016/s0168-3659(02)00050-0, PMID 11992680.
36. Shinoda K, Lindman B. Organized surfactant systems: microemulsions. Langmuir. 1987;3(2):135-49. doi: 10.1021/la00074a001.
37. Kreilgaard M, Pedersen EJ, Jaroszewski JW. NMR characterization and transdermal drug delivery potential of microemulsion systems. J Control Release. 2000;69(3):421-33. doi: 10.1016/s0168-3659(00)00325-4, PMID 11102682.
38. Perez GRM, Solis VR. Anti-inflammatory and wound healing potential of *Prosthechea michuacana* in rats. Pharmacogn Mag. 2009;4:219-25.
39. Lodhi S, Pawar RS, Jain AP, Jain A, Singhai AK. Effect of *Tephrosia purpurea* (L) Pers. on partial thickness and full thickness burn wounds in rats. J Complement Integr Med. 2010;7(1):1-15. doi: 10.2202/1553-3840.1344.
40. Xu HX, Lee SF. Activity of plant flavonoids against antibiotic-resistant bacteria. Phytother Res. 2001;15(1):39-43. doi: 10.1002/1099-1573(200102)15:1<39::aid-ptr684>3.0.co;2-r, PMID 11180521.